Mechano-chemical ageing of PES/PVP ultrafiltration membranes used in drinking water production

B. Pellegrin, E. Gaudichet-Maurin and C. Causserand

ABSTRACT

In water treatment by microfiltration and ultrafiltration, a major concern is the integrity loss or failure of membrane induced by onsite operations, potentially leading to permeate water contamination. This study aims to provide a better understanding of the phenomena responsible for membrane damage by analyzing its causes and effects. The role of sodium hypochlorite exposure conditions and the impact of mechanical stress on membrane characteristics were investigated. Monitoring of hydraulic response, mechanical properties and the evolution of the chemical structure showed, on multiple scales, strong indications of membrane chemical degradation, involving radical mechanisms, accelerated by tensile stress application.

Key words ageing, hypochlorite cleaning, mechanical stress, PES, PVP, ultrafiltration membrane

B. Pellegrin
C. Causserand (corresponding author)
Université de Toulouse, INPT, UPS,
Laboratoire de Génie Chimique,
118 Route de Narbonne, 31062 Toulouse,
France
E-mail: *caussera@chimie.ups-tlse.fr*

B. Pellegrin
C. Causserand
CNRS, Laboratoire de Génie Chimique, UMR 5503,
31062 Toulouse,
France

E. Gaudichet-Maurin
Véolia Environnement Recherche et Innovation,
Ch. de la Digue, 78603 Maisons-Laffitte,
France

INTRODUCTION

Due to their high efficiency in the removal of particles, bacteria and viruses with limited energy consumption, microfiltration (MF) and ultrafiltration (UF) are attracting increasing attention throughout the world. During the past decades, UF has become extensively used in the production of high quality drinking water. However, it is now well established that fouling, resulting from reversible or irreversible adsorption, accumulation and cake build-up of solutes at the membrane surface, is one of the major drawbacks of membrane filtration processes. Occurring gradually with filtration time, fouling induces a decrease in permeate flux leading to lessened energy efficiency, drastically impairing membrane performances (Marshall *et al.* 1993; Bacchin *et al.* 2006). Thus, during onsite operation, back-washing and chemical cleaning are periodically carried out to get rid of hydraulically and chemically reversible fouling and ensure proper membrane function. As major water treatment facilities appear to be subjected to membrane failure and integrity loss on a quite regular basis (Gijsbertsen-Abrahamse *et al.* 2006), the impact of industrial washing on membrane properties has recently become a key issue. Among the wide range of cleaning chemicals available, due to its antibacterial/oxidizing properties, sodium hypochlorite (NaOCl) is one of the most effective and, therefore, commonly used disinfection/cleaning agents in water purification (Porcelli & Judd 2010).

Polyethersulfone (PES), exhibiting good chemical resistance, mechanical properties and thermal stability, appears as a first-choice polymeric material for UF hollow fibers formulation. The PES monomer unit comprises alternating sulfonyl (–SO_2–) and ether (–O–) functional groups connected together by phenylene rings (Figure 1(a)). PES being a relatively hydrophobic polymer, the inclusion of more hydrophilic polymers such as poly(N-vinylpyrrolidone) (PVP) (Figure 1(b)) has become a standard method to obtain so called 'hydrophilized' PES membranes which provide lower water resistance and propensity for fouling than virgin PES membranes. Addition of specific amounts of PVP in the PES dope solution also allows pore size and distribution tuning of membranes prepared by non-solvent-induced phase separation (NIPS) (Ulbricht 2006).

In 1995, Wienk *et al.* reported an increase of pure water flux through PES/PVP membranes due to PVP chain scission during membrane immersion in a 4,000 ppm NaOCl

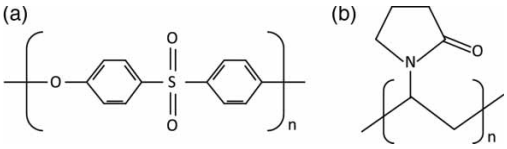

Figure 1 | Molecular structures of polyethersulfone (a) and poly(N-vinylpyrrolidone) (b).

solution under stirring (Wienk *et al.* 1995). Later on, Wolff and Zydney and Qin *et al.* confirmed the permeability augmentation (up to five-fold increase) observed by Wienk *et al.* and showed an alteration of the retention properties of polysulfone (PS)/PVP and PES/PVP blended membranes soaked in NaOCl solutions (Qin & Wong 2002; Wolff & Zydney 2004; Qin *et al.* 2005). These studies considered such an effect as an advantage and suggested hypochlorite contact to be used as an efficient post-treatment for the elimination of excess PVP from the membrane pores.

Its aromatic structure, together with its fully amorphous nature and the absence of labile hydrogen, confers a relatively high thermal and chemical stability to PES (Mark 2004). Therefore, PES is considered as highly tolerant to oxidants and only little information is available regarding the effect of hypochlorite on PES polymer. However, different authors recently reported a degradation of PES or PES/PVP membrane properties when exposed to hypochlorite. Temperature and pH dependent PES chain scission was suggested to be responsible for this degradation. From X-ray photoelectron spectroscopy (XPS) and attenuated total reflection – Fourier transform infrared (ATR-IR) spectral analysis, Thominette *et al.* (2006) reported the formation of sulfonate groups and Arkhangelsky *et al.* (2007a, b) underlined the decrease of the 1,485 cm^{-1} band, attributed to C-S vibrations. Based on these observations, they both proposed a partial PES chain scission mechanism at the ether–sulfone linkage, leading to the formation of $PhSO_3^-$. A study by Yadav *et al.* (2009) found, from field emission scanning microscopy/energy dispersive X-ray analysis (FESEM/EDX) measurements, that long-term exposure of the PES membrane to hypochlorite at pH 9 leads to incorporation of chlorine at the membrane surface. The presence of chlorine was not observed for pH 12 hypochlorite-exposed membranes and sodium was detected neither at pH 9, nor at pH 12. From the PES cleavage mechanism of Thominette *et al.* (2006), Yadav *et al.* (2009) proposed a modified chain scission mechanism occurring preferentially at pH 9 and leading to backbone cleavage into two different parts: one end terminated by a sulfonic acid group ($PhSO_3H$) and the other terminated by a phenyl chloride group (PhCl). In a second study, Yadav & Morrison (2010) focused on flux variations of PES membranes exposed to hypochlorite solutions over a pH range of 9 to 12. It was found that hypochlorite exposure significantly increased the pure water flux as well as the interactions between membrane surface and proteins, leading to greater fouling. The effects of hypochlorite on membrane water flux and protein adsorption were found to be more severe as the pH of the hypochlorite solution was lowered.

The aim of this work was to provide further understanding of hypochlorite effects, over a range of exposure times and pH, on the macroscopic and filtration properties of PES/PVP UF hollow fibers and assign the modifications to a molecular level. An accelerated ageing process at the laboratory scale combining hypochlorite exposure and axial tensile stress, representative of onsite PES/PVP membrane degradation due to chlorine exposure together with pressure conditions was developed. Hydraulic response, mechanical properties and changes in the chemical structure were monitored for a wide range of conditions. Systematic analysis and comparison of onsite and artificially aged samples were undertaken.

METHODS

Materials

PES/PVP hollow fibers were extracted from a commercially available UF module, widely used for drinking water production and provided by Véolia Environnement. According to manufacturer's data, the membranes are composed of 'hydrophilized' PES, with an internal diameter of 0.8 mm, an external diameter of 1.3 mm and a molecular weight cut-off (MWCO) of 150 kDa. These membranes are to be used in an inside-out filtration configuration. After extraction from the module, the membranes were stored in a 1 g L^{-1} sodium bisulfite ($Na_2O_4S_2$ – Technical grade 85%, Sigma-Aldrich, USA) solution at 5 °C to avoid bacterial proliferation. Samples were systematically soaked in ultra-pure water for 1 h before use. All aqueous solutions were prepared with deionized ultra-pure water ($\rho = 18.2$ MΩ cm) obtained with a PURELAB Maxima system (ELGA LabWater's, UK). Dissolution of

membranes for size exclusion chromatography (SEC) measurements was carried out in N,N-dimethylmethanamide (DMF – Analytical grade, Carlo Erba Reagents, France).

Ageing protocols

Accelerated ageing experiments were all performed by soaking the membranes in 350 ppm (mg L^{-1}) total free chlorine solutions, corresponding to the range commonly used onsite for chemical cleaning process. Hypochlorite solutions were obtained by dilution of a commercial NaOCl solution (NaOCl 9.8 wt% – La Croix, France). Total free chlorine concentration ([TFC]) was monitored using the so called DPD method (EPA-approved method 4500 CI G): reaction of chlorine-containing samples with N,N-diethyl-p-phenylenediamine sulfate in the presence of a specific buffer producing a pink colored compound, measured at 520 nm using a spectrophotometer (DR/2400, Hach, USA). The pH of the soaking solutions was adjusted to 6, 8 and 11. The pH 8 and 11 conditions correspond to approximate onsite back-washing and chemical cleaning processes respectively. In addition, pH 6 was also investigated, as it corresponds to the prevalence of the HClO species, whereas pH 11 corresponds to ClO^- species predominance and pH 8 leads to coexistence of both HClO and ClO^- species in solution. The pH of the soaking solutions was adjusted by addition of concentrated sulfuric acid (H_2SO_4 – Analytical grade 95%, VWR Prolabo, France) and sodium hydroxide (NaOH – Analytical grade, Carlo Erba Reagents, France). As [TFC] and pH were found to decrease with time, constant [TFC] (±30 ppm) and pH (±0.2) were maintained by daily adjustment of the soaking solutions. Samples were systematically soaked in ultra-pure water for 2 h and stored in a 1 g L^{-1} $Na_2O_4S_2$ solution at 5 °C after each accelerated ageing experiment.

Static accelerated ageing was conducted on membranes at ambient temperature (20 ± 2 °C), in NaOCl solutions at a [TFC] of 350 ppm, for pH values ranging from 6 to 11, and for exposure times ranging from 1 h to 41 days. Control membrane samples were similarly soaked in ultra-pure water for up to 41 days. Another set of NaOCl ageing experiments was performed using the conditions mentioned above with the addition of 2 g L^{-1} of 2-methylpropan-2-ol (*t*BuOH – HPLC grade 99.5%, Sigma-Aldrich, USA) as a radical scavenger in the soaking solution.

A similar NaOCl ageing protocol was applied to membranes subjected to the impact of a specific load (Figure 2(a)). Connection of an adequately chosen weight (mass $m = 380$ g, density $\rho = 2{,}330$ kg m^{-3}) to the end of a fiber generates an applied constant axial tensile stress of $\sigma_a = 2.6$ MPa. The axial stress applied was arbitrarily chosen to be located on the upper part of the elastic domain of the membrane stress–strain curve (Figure 2(b)).

Usually, for onsite operation, membranes are periodically subjected to free chlorine contact during back-washing and chemical cleaning. Depending on the characteristics of the water treated, water treatment facility operators may use NaOCl solutions with a [TFC] of up to 20 ppm during up to 5 min for back-washing and with a [TFC] up to 400 ppm for up to 2 h for chemical cleaning. Frequencies may reach, for back-washing and chemical cleaning respectively, 1 per 6 h of membrane operation and 1 per month of membrane

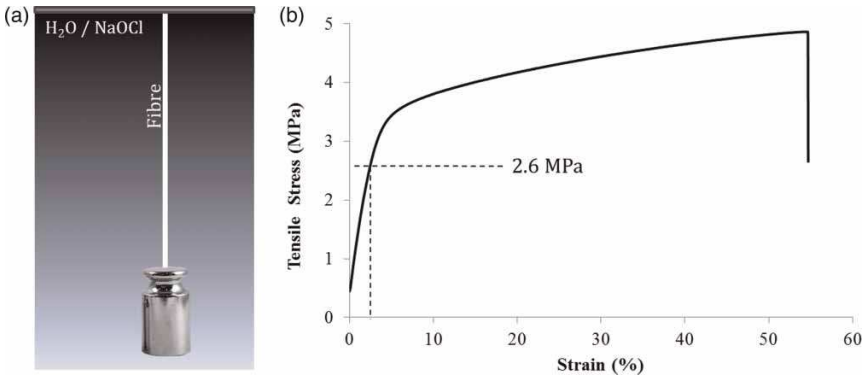

Figure 2 NaOCl ageing coupled to axial stress schematic protocol (a). Example of a tensile stress–strain curve of a pristine PES membrane (b).

operation. Even if membranes are only periodically in contact with hypochlorite, the combined amount of NaOCl in contact with membranes can be expressed as a total dose. Hypochlorite dose will then refer to the [TFC] of the NaOCl soaking solution, multiplied by the sample NaOCl exposure time. For convenience, NaOCl dose is expressed in g h L^{-1}, which is the most appropriate unit for the range of doses studied. Based on the most severe conditions membranes might encounter onsite, it is possible to assess an approximate equivalence between onsite operation time and laboratory soaking time (Table 1).

Additionally, similar PES/PVP membranes extracted from operated industrial modules were gathered and similarly analyzed. Systematic comparison with the laboratory aged samples was carried out.

Membrane characterization

Permeability measurements

Pure water flux measurements were carried out with a cross-flow filtration set-up at controlled temperature of 20 ± 2 °C on virgin membranes and on samples after ageing in various conditions. Ultra-pure water was forced to permeate from the inside to the outside of a laboratory scale module comprising 15 hollow fibers (220 ± 5 mm length). The trans-membrane pressure (ΔP) was applied by adjusting a pressure valve at the retentate side. ΔP was varied from 0.05 to 0.14 MPa and taken as the average of the feed pressure and the retentate side pressure readings, upstream of the pressure valve. To overcome the membrane compaction impact, each module tested was first subjected to cross-flow filtration of ultra-pure water at maximal pressure of 0.14 MPa until pure water flux stabilization (20 min). The pure water permeability (L_p/μ_{20} in L h^{-1} m^{-2} bar^{-1}, with L_p the permeability coefficient and μ_{20} the fluid viscosity at 20 °C) was calculated from the Darcy law.

$$J_T = \frac{L_p}{\mu_T}\Delta P$$

where J_T is the flux density (in L h^{-1} m^{-2}) calculated using the inner surface area of the membranes and μ_T the fluid viscosity for the experiment temperature.

The flux density J_T was systematically corrected back to J_{20} using the empirical Arrhenius law of the fluid viscosity variation as a function of the temperature.

$$J_{20} = J_T\frac{\mu_T}{\mu_{20}} = J_T \exp\left(\frac{E_0}{RT} - \frac{E_0}{293R}\right)$$

where E_0 is the activation energy of the fluid (for water E_0 = 15,675 J mol^{-1} (Schweitzer 1988)), R the universal gas constant and T the temperature of the experiment.

L_p/μ_{20} was then taken as the slope value of the linear regression between ΔP and J_{20} values.

Scanning electron microscopy (SEM)

SEM images of the inner active layer of membranes were recorded using a JEOL JSM 6700F field emission gun-SEM. Prior to analysis, samples were cut open axially using a scalpel blade, dried in a vacuum oven at room temperature for at least 1 h and a 5 nm silver layer was sputtered on the sample surface. Note that cross-section images were also recorded using the same protocol on liquid nitrogen fractured samples, to check internal and external membrane diameters. To obtain an accurate representation of membrane surface morphology, a set of six to ten images was recorded for each condition analyzed.

Tensile strain at break measurements

Tensile tests were performed on a Instron 3342 series tensile apparatus fitted with tailor-made grips for the hollow fiber geometry to avoid stress concentration. The initial distance between

Table 1 Correlation between membrane onsite operation time (for the most severe onsite conditions of use) and laboratory soaking time (for a [TFC] of 350 ppm)

24 h/24 h onsite operation time			Laboratory NaOCl soaking time	
(months)	(years)	Hypochlorite dose (g h L^{-1})	(h)	(days)
1	–	1	2.9	–
6	–	6	17.1	–
12	1	12	34.3	1.4
24	2	24	68.6	2.9
126	10.5	126	360	15
235.2	19.6	235.2	672	28

grips was fixed to 110 mm and samples were extended at a constant elongation rate of 100 mm min^{-1}. Young's modulus E, tensile stress at break σ_R and elongation at break ε_R were calculated from the experimental stress–strain curves. A set of eight samples was analyzed for each condition investigated.

Attenuated total reflection - Fourier transform infrared (ATR-IR) spectroscopy

Infrared spectra of the inner active layer of membranes were recorded using a Thermo-Nicolet Nexus 670 fitted with a DTGS detector and a diamond ATR crystal. Spectra were obtained by summing sixteen scans between 4,000 and 400 cm^{-1} with a resolution of 4 cm^{-1}. Spectral analysis was performed on OMNIC® software. Membrane samples were cut open axially to gain access to the inner active layer for analysis. Prior to analysis, samples were systematically dried in a vacuum oven for 2 h at 50 °C and shortly stored in a desiccator. All absorbance values were normalized back to the 1,150 cm^{-1} band, which corresponds to $-SO_2-$ symmetric stretching. The absorbance values presented are an average of at least four samples.

Size exclusion chromatography (SEC)

SEC chromatograms of membrane material dissolved in DMF (5 g L^{-1}) were performed using a refractometer fitted apparatus connected to two Tosoh Bioscience columns (TSK-Gel Alpha 3000 and 5000). Analyses were performed using a DMF mobile phase, at a constant flow rate of 1 mL min^{-1}. The detector was calibrated with polyethylene glycol standards. The peak corresponding to the elution time of PES was then analyzed to obtain molecular mass distribution of PES. From a set of three pristine membrane samples standard deviation on weight average molar mass ($\overline{M}_w$) and number average molar mass ($\overline{M}_n$) of PES was evaluated to 2,200 and 630 g mol^{-1} respectively.

X-ray photoelectron spectroscopy (XPS)

XPS analyses of the inner active layer of the membranes were performed using an Escalab 250 (Thermo Electron) device with Al Kα radiation as the monochromatic X-ray source (1,486.6 eV). XPS measurements were repeated on three distinct samples for each condition analyzed. Prior to active layer analysis, the same sample preparation protocol as for ATR-IR measurements was applied.

RESULTS AND DISCUSSION

Ageing by static immersion in NaOCl

Hydraulic response

Figure 3 presents membrane permeability versus hypochlorite dose at pH 8. A drastic increase in pure water flux was observed at very low doses, followed by a quasi-stabilization at approximately twice the initial L_p/μ_{20} value. Pure water permeability (L_p/μ_{20}) is plotted against NaOCl dose and pH in Table 2. As expected, contact with hypochlorite solution leads to an increase of pure water flux through membranes. For all pH values studied, membrane

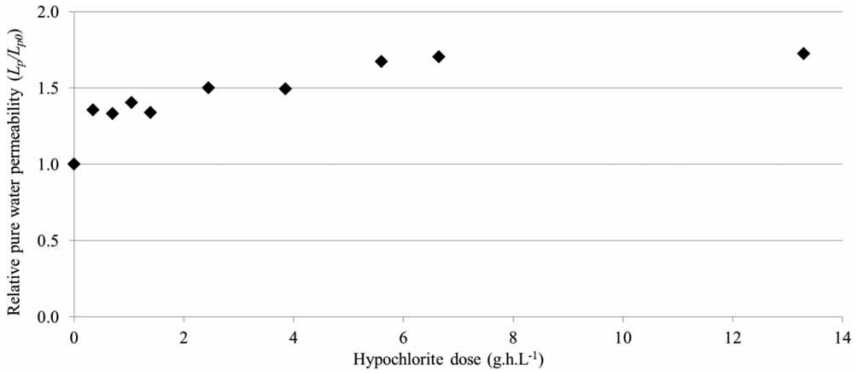

Figure 3 Relative pure water permeability versus hypochlorite dose for static immersion in 350 ppm NaOCl solution at pH 8.

Table 2 L_p/μ_{20} of membrane samples soaked in ultra-pure water and 350 ppm NaOCl solutions for 360 h (126.0 g h L^{-1}) and for 672 h (235.2 g h L^{-1})

	Pure water permeability L_p/μ_{20} (L h^{-1} m^{-2} bar^{-1})						
Soaking time (h)	**Ultra-pure water**	**NaOCl pH 6**	**NaOCl pH 7**	**NaOCl pH 8**	**NaOCl pH 9**	**NaOCl pH 10**	**NaOCl pH 11**
0	514[a]	514[a]	514[a]	514[a]	514[a]	514[a]	514[a]
360	560	711	781	962	950	905	827
672	538	984	990	1,070	1,160	1,127	1,014

[a]Initial pure water permeability is reported as the average permeability of six laboratory-scaled modules containing new fibers and presents a standard deviation of 52 L h^{-1} m^{-2} bar^{-1}.

permeability showed an increase, reaching 1.9 to 2.2 times the initial pure water permeability after exposure to a hypochlorite dose of 235.2 g h L^{-1}. For high exposure doses, the increase of pure water flux did not show clear dependence on the pH of chlorine solutions.

Surface morphology

NaOCl exposure impact on the inner active layer was confirmed by direct microscopic observation. Figure 4 presents SEM images of sample inner surfaces exposed to different chlorine doses at pH 8. It appears that surface morphology is substantially modified for low doses, which supports the change in the pure water permeability observed. The same observations were made for pH 6 and 11.

Mechanical properties

The effects of hypochlorite exposure on the overall mechanical performances of the fibers were monitored by tensile testing. It appeared, for all pH and NaOCl doses investigated, that Young's modulus E was not significantly affected. The envelope of the stress–strain curves remained essentially unchanged in the elastic domain and in the early stages of plastic deformation. Changes occurred at the final extremity of the plastic domain. Both tensile stress at break σ_R and elongation at break ε_R decreased as hypochlorite dose was increased. In other words, fracture occurred sooner, meaning that membrane ductility decreased for aged samples. In such cases of material embrittlement, elongation at break ε_R is the most pertinent parameter to monitor.

Figure 5(a) presents the results obtained for tensile strain (elongation) at break ε_R as a function of the hypochlorite dose and the pH of the soaking solution. It clearly appears that membranes underwent the most severe degradation for slightly basic pH value (pH 8). As a conclusion, for high NaOCl doses, in opposition to pure water permeability, the variation of the mechanical properties of aged membranes strongly depends on the pH of the hypochlorite solution.

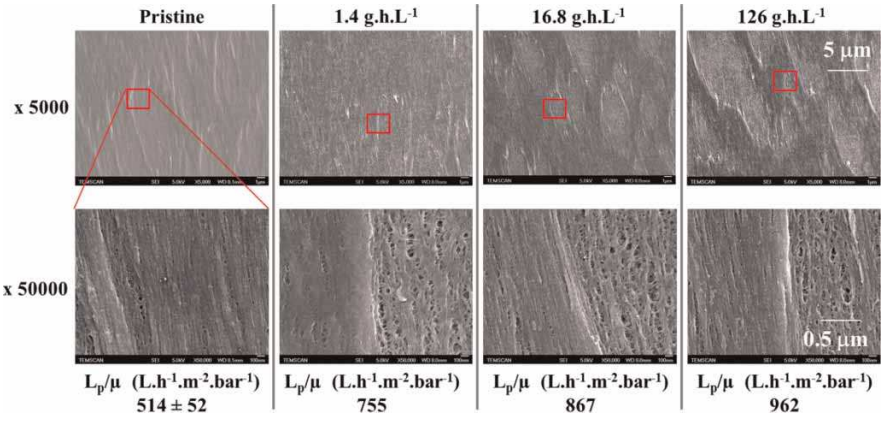

Figure 4 SEM images of inner surface of membranes as a function of hypochlorite dose at pH 8.

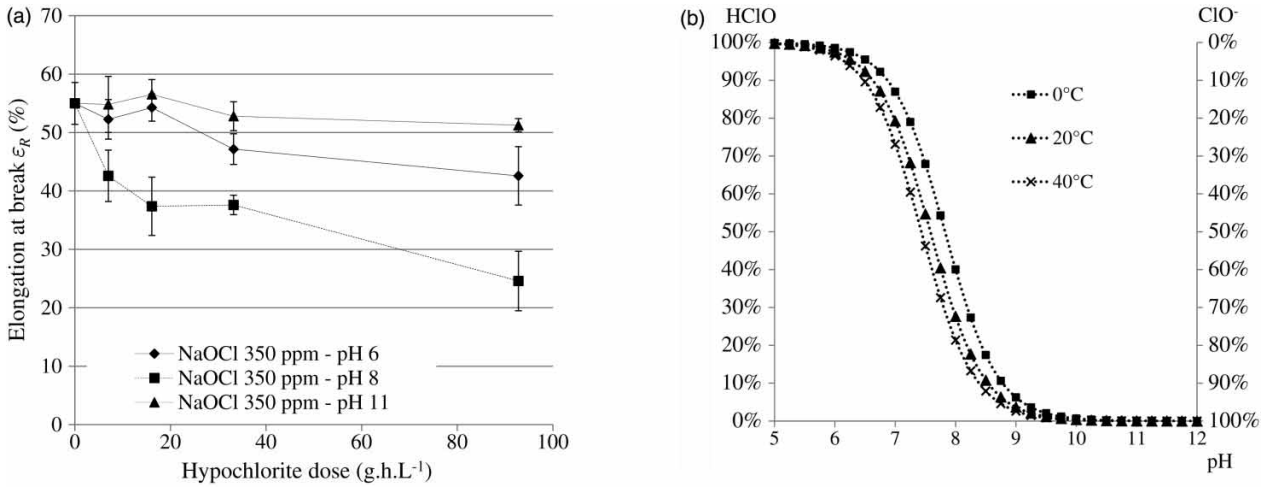

Figure 5 Elongation at break ε_R as a function of pH and hypochlorite dose (a); HClO/ClO$^-$ species dissociation curve (b).

If we refer to the chlorine dissociation curve (Figure 5(b)), the region $7 < \text{pH} < 8$ is where HClO and ClO$^-$ coexist (White 1999). Thus, this pH range corresponds to suitable conditions for the following reaction (Wienk *et al.* 1995):

$$\text{HClO} + 3\text{ClO}^- \rightarrow 3\text{Cl}^- + \text{ClO}^\bullet + \text{O}_2 + \text{HO}^\bullet$$

This reaction, reported by Wienk *et al.* (1995) thus leads to the formation of ClO$^\bullet$ and HO$^\bullet$ radicals. Fibers embrittlement occurring more severely at pH 8 may then mainly correspond to a radical attack of the membrane structural polymers.

In order to validate this hypothesis, another set of static hypochlorite ageing tests was performed with the addition of 2-methylpropan-2-ol (*t*BuOH) used as a radical scavenger in excess in the soaking solution. Experiments were conducted at pH 6 and 8. Membrane mechanical properties were similarly evaluated by monitoring the elongation at break ε_R. The results are presented in Figures 6(a) and 6(b). Addition of *t*BuOH to hypochlorite soaking solution at pH 6 had no impact on the kinetics

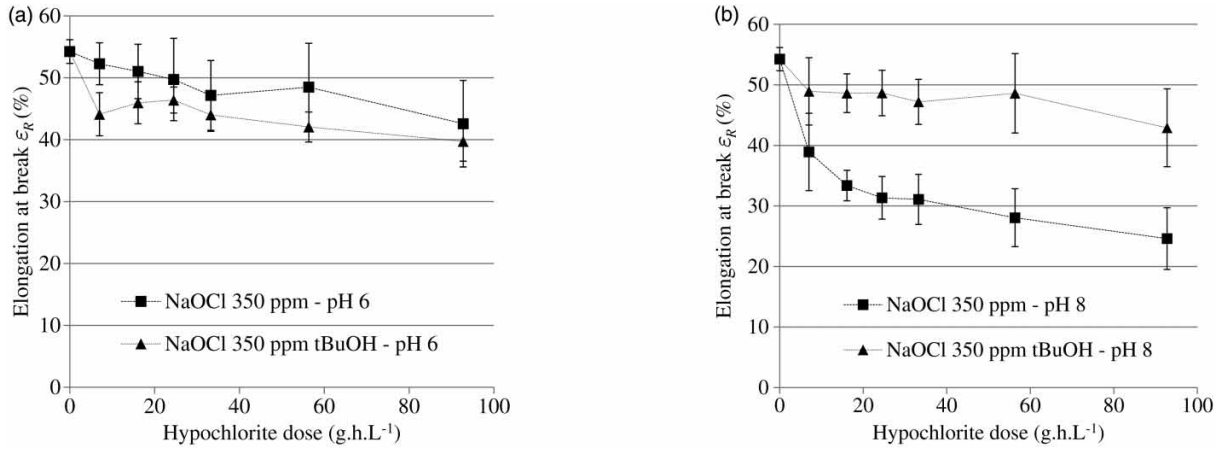

Figure 6 Membrane elongation at break ε_R as a function of hypochlorite dose when exposed to 350 ppm NaOCl solutions, with and without 2-methylpropan-2-ol (*t*BuOH), at pH 6 (a) and pH 8 (b).

of the decrease of elongation at break ε_R, whereas it substantially slowed down embrittlement of membranes soaked in hypochlorite solution at pH 8. Moreover, the embrittlement rate of membranes exposed to NaOCl/*t*BuOH at pH 8 appeared to be similar to the embrittlement rate of membranes exposed to NaOCl at pH 6. Those results provide indirect evidence for radical induced degradation of membrane material at pH 8.

Chemical analysis

To follow the changes occurring at a molecular level in the membrane permeability and mechanical properties on exposure to chlorine, molar mass distribution of PES of pristine and hypochlorite exposed samples were characterized by SEC. Weight average molar mass ($\overline{M}_w$) and number average molar mass ($\overline{M}_n$) of PES of membranes exposed to a set of hypochlorite doses at pH 8 are presented in Table 3. SEC analyses did not reveal any significant variation of the mass distribution of PES, even at very high NaOCl exposure doses. In other words, no reticulation or chain scission phenomena were detected in the structural polymer of the membrane (i.e. PES).

Degradation of the membrane active layer was also characterized by ATR-IR and XPS analyses. The depth analyzed by both methods was approximately 1–4 μm and 1–10 nm respectively. Spectra for pristine and hypochlorite-exposed samples (Figure 7) exhibited no major evolution but a significant decrease of the 1,674 cm^{-1} band for all pH studied. 1,674 cm^{-1} IR band is assigned to the stretching vibration of the C=O bond in the PVP amide unit (Hassouna *et al.* 2009). This decrease suggests lowered PVP levels on the membrane surface when exposed to hypochlorite, which was confirmed by XPS measurements. As PES and PVP monomer units carry respectively one single sulfur (S) and one nitrogen (N), the N/S atomic ratio obtained from XPS analysis may be considered as a direct evaluation of the fraction of PVP present on the extreme surface of the membrane inner layer. Table 4 presents the atomic percentages

Table 3 $\overline{M}_w$ and $\overline{M}_n$ values of PES of membranes immerged into hypochlorite solutions at pH 8

Hypochlorite dose (g h L^{-1})	0	29.4	67.2	235.2	345
$\overline{M}_n$ (g mol^{-1})	15,390	15,334	15,835	15,407	15,088
$\overline{M}_w$ (g mol^{-1})	38,682	39,620	40,944	38,810	37,761
$\overline{M}_w/\overline{M}_n$	2.51	2.58	2.58	2.52	2.50

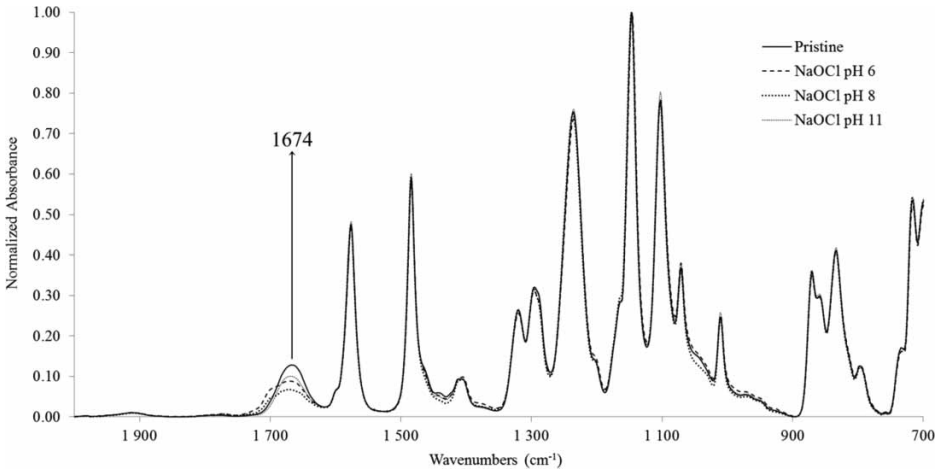

Figure 7 ATR-IR spectra of the inner surface of pristine membranes and of membranes exposed to a hypochlorite dose of 126 g h L^{-1} at pH 6, 8 and 11.

Table 4 Elemental content of hypochlorite-treated membrane inner surfaces detected by XPS

	Elemental concentration (%)				Ratio
	S 2p	C 1s	N 1s	O 1s	N/S
Pristine	6.1 ± 0.2	73.8 ± 0.3	2.7 ± 0.2	17.3 ± 0.2	0.44
84 g h L^{-1} – pH 8	6.4 ± 0.1	71.8 ± 0.3	1.9 ± 0.05	19.1 ± 0.2	0.30
84 g h L^{-1} – pH 11	6.3 ± 0.05	73.7 ± 0.2	2.3 ± 0.1	17.5 ± 0.2	0.36

obtained by XPS analysis on the active layer of pristine membranes and membranes exposed to hypochlorite. It clearly shows a decrease of the N/S atomic ratio for hypochlorite-exposed membranes, especially at pH 8.

ATR-IR and XPS analyses both revealed strong indications of degradation and loss of PVP in the membrane active layer. As membrane pure water permeability is mainly governed by membrane active layer properties, we plotted (Figure 8) the pure water permeability of aged samples versus the normalized 1,674 cm^{-1} band intensity, characterizing the PVP content of the membrane active layer. This figure presents a compilation of the data collected at pH 6, 8 and 11, for a wide range of hypochlorite doses. It exhibits a linear correlation between the amount of PVP detected on the membrane surface by ATR-IR and pure water flux.

From the above observations, it can reasonably be thought that the changes occurring in membrane permeability and mechanical properties on exposure to chlorine may be largely induced by PVP degradation and departure from the membrane material. No evidence of the hypothesis of the PES chain scission proposed in the literature (Thominette *et al.* 2006; Arkhangelsky *et al.* 2007a, b; Yadav *et al.* 2009) was observed. In PES/PVP blended membranes, PES chain breaks appear to be responsible for macroscopic membrane property alterations to a much lesser extent than PVP degradation and loss.

Ageing by static NaOCl immersion under constant mechanical stress

Autopsy of similar PES/PVP membranes extracted from an operated industrial module was performed. The membranes had been used in a French plant for karstic water filtration. The module operated 6 h per day, for approximately 5 years. Presenting too many broken fibers to be fixed, it was discarded in 2011. Knowing the history of membrane cleaning, it was possible to calculate the approximate hypochlorite dose the membranes had been subjected to, which

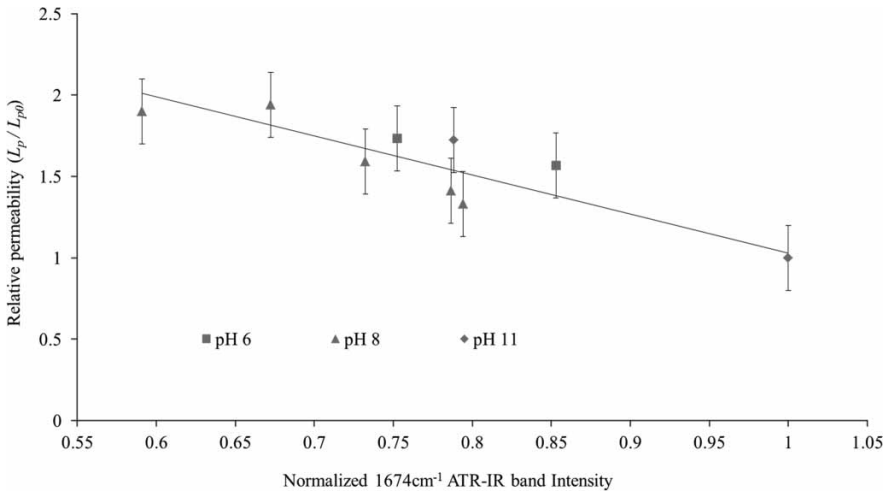

Figure 8 Pure water permeability versus normalized 1,674 cm^{-1} ATR-IR band intensity.

would be about 10 g h L^{-1}. Mechanical testing was performed on the membranes (not presented) and showed an elongation at break ε_R lowered to a level corresponding to an observed impact during laboratory hypochlorite soaking obtained for doses five- to ten-fold higher. From this observation, it can be assumed that hypochlorite is far from being the only factor impacting membrane degradation and failure during onsite operation.

In light of these results, hypochlorite soaking of new membranes was combined with constant axial stress application, as explained in the protocol described earlier (Figure 2). In most cases, industrial hypochlorite cleaning is performed in filtration or in back-washing mode, and thus, a transmembrane pressure (ΔP) is applied. ΔP can be interpreted as a radial tensile stress applied to membranes. Even though the set-up reported in Figure 2 generates axial stress, it was thought to provide information reflecting, to some extent, the combined impact of ΔP and hypochlorite exposure on membranes. The elongation at break ε_R of membranes exposed to a set of treatments is reported in Figure 9. Firstly axial tensile stress was applied to membrane samples immerged in water (Samples #2). Very little impact on elongation at break ε_R was observed. Another set of samples was soaked in a 350 ppm hypochlorite solution at pH 8, free of stress (Samples #3). Lowering of ε_R was observed, coherently with the evolution previously reported for static hypochlorite exposure at pH 8. These two protocols were applied one after the other to another set of samples (Samples #4), meaning that the samples were subsequently hypochlorite-treated and subjected to tensile stress in water. Results very similar to those of sample set #3 were obtained. Finally, a last set of samples (Samples #5) was immerged in hypochlorite solution under constant stress. Elongation at break appeared to be lowered to about 30% of the initial ε_R. This last result clearly demonstrates a synergistic effect of hypochlorite combined to application of tensile stress. In other words, ΔP is very likely to accelerate the membrane degradation induced by hypochlorite exposure during onsite cleaning.

CONCLUSIONS

A systematic study of PES/PVP hollow fiber membrane degradation following contact with NaOCl was undertaken. The results showed that the cleaning process substantially affects membrane performance. Firstly, for all values of pH studied, PVP appeared to be dislodged from the PES membrane matrix, leading to a drastic increase in pure water flux. Secondly, for slightly basic conditions, $ClO^{\bullet}$ and $HO^{\bullet}$ radicals play a significant role in the membrane degradation, impacting the mechanical properties. Chemical analyses did not bring direct evidence of PES chemical attack, but showed strong indications of PVP degradation and release from the PES matrix. In conclusion, chemical ageing of PES/PVP blended membranes in contact with hypochlorite solution is mainly due to PVP degradation even though PVP only accounts for a small proportion of the membrane material. In addition, it was demonstrated that the ΔP

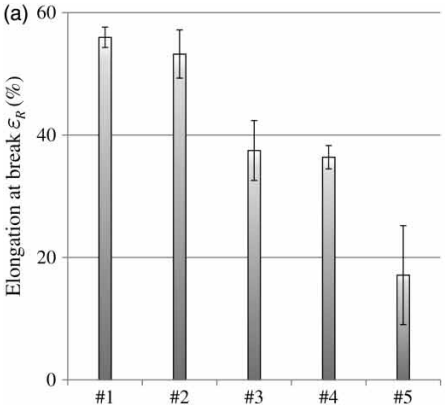

(b)

	Treatments applied to membranes			
	Water 5 days	NaOCl 42 g.h.L^{-1} pH 8	Water – 5 days Under constant stress	NaOCl 42 g.h.L^{-1} pH 8 Under constant stress
#1	X	-	-	-
#2	-	-	X	-
#3	-	X	-	-
#4	-	X	X	-
#5	-	-	-	X

Figure 9 Elongation at break ε_R as a function of the treatment applied to membranes.

applied during onsite hypochlorite cleaning may further accelerate chemical degradation of membranes at pH 8.

REFERENCES

Arkhangelsky, E., Kuzmenko, D. & Gitis, V. 2007a Impact of chemical cleaning on properties and functioning of polyethersulfone membranes. *J. Membr. Sci.* **305**, 176–184.

Arkhangelsky, E., Kuzmenko, D., Gitis, N. V., Vinogradov, M., Kuiry, S. & Gitis, V. 2007b Hypochlorite cleaning causes degradation of polymer membranes. *Tribol. Lett.* **28**, 109–116.

Bacchin, P., Aimar, P. & Field, R. W. 2006 Critical and sustainable fluxes: theory, experiments and applications. *J. Membr. Sci.* **281**, 42–69.

Gijsbertsen-Abrahamse, A. J., Cornelissen, E. R. & Hofman, J. A. M. H. 2006 Fiber failure frequency and causes of hollow fiber integrity loss. *Desalination* **194**, 251–258.

Hassouna, F., Therias, S., Mailhot, G. & Gardette, J. L. 2009 Photooxidation of poly(N-vinylpyrrolidone) (PVP) in the solid state and in aqueous solution. *Polym. Degrad. Stab.* **94**, 2257–2266.

Mark, H. F. 2004 *Encyclopedia of Polymer Science and Technology*, 3rd edn. Wiley-Interscience Publication, USA, pp. 1–26.

Marshall, A. D., Munro, P. A. & Trägardh, G. 1993 The effect of protein fouling in microfiltration and ultrafiltration on permeate flux, protein retention and selectivity: a literature review. *Desalination* **91**, 65–108.

Porcelli, N. & Judd, S. 2010 Chemical cleaning of potable water membranes: a review. *Separ. Purif. Tech.* **71**, 137–143.

Qin, J. J. & Wong, F. S. 2002 Hypochlorite treatment of hydrophilic hollow fiber ultrafiltration membranes for high fluxes. *Desalination* **146**, 307–309.

Qin, J. J., Oo, M. H. & Li, Y. 2005 Development of high flux polyethersulfone hollow fiber ultrafiltration membranes from a low critical solution temperature. *J. Membr. Sci.* **247**, 137–142.

Schweitzer, P. A. 1988 *Handbook of Separation Techniques for Chemical Engineers*, 2nd edn. McGraw-Hill, USA, pp. 2–98.

Thominette, F., Fanault, O., Gaudichet-Maurin, E., Machinal, C. & Schrotter, J. C. 2006 Ageing of polyethersulfone ultrafiltration membranes in hypochlorite treatment. *Desalination* **200**, 7–8.

Ulbricht, M. 2006 Advanced functional polymer membranes. *Polymer* **47**, 2217–2262.

White, G. C. 1999 *Handbook of Chlorination and Alternative Disinfectants*, 4th edn. Wiley-Interscience Publication, USA, pp. 212–287.

Wienk, I. M., Meuleman, E. E. B., Borneman, Z. & Boomgaard, T. 1995 Chemical treatment of membranes of a polymer blend: mechanism of the reaction of hypochlorite with poly(vinyl pyrrolidone). *J. Polym. Sci.* **33**, 49–54.

Wolff, S. H. & Zydney, A. L. 2004 Effect of bleach on the transport characteristics of polysulfone hemodialyzers. *J. Membr. Sci.* **243**, 389–399.

Yadav, K. & Morison, K. R. 2010 Effects of hypochlorite exposure on flux through polyethersulfone ultrafiltration membranes. *Food Bioprod. Process.* **88**, 419–424.

Yadav, K., Morison, K. R. & Staiger, M. P. 2009 Effects of hypochlorite treatment on the surface morphology and mechanical properties of polyethersulfone ultrafiltration membranes. *Polym. Degrad. Stab.* **94**, 1955–1961.